Progress In Electromagnetics Research M, Vol. 98, 1–10, 2020

Shielding Effectiveness of a Closed Cylindrical Surface Simulated by N Dielectric Coated Conducting Strips

Hassan Ragheb*

Abstract—The paper aims at studying the shielding effectiveness of a closed cylindrical surface simulated by N dielectric coated conducting strips. The far fields of an electric line source in the presence of the simulated surface and in the absence of the surface were calculated, and the ratio between them represents the shielding effectiveness produced around the surface. The solution of the problem was developed based on full wave analysis. Numerical results are presented for circular and square cross-sectional cylindrical surfaces. Comparison with the published data for the radiation from slotted circular cylinder showed excellent agreement. Other useful results for shielding effectiveness are furnished.

1. INTRODUCTION

Electromagnetic shielding is needed in many applications, such as the case for electronic equipment, the room containing sensitive electronic apparatus or preventing electromagnetic waves from propagating in pre-specified direction. In most applications, one or more openings may exist. Therefore, shielding effectiveness is an important factor to calculate in order to study the shielding performance. Accordingly, extensive investigations have been introduced for the calculation of the shielding effectiveness. In general, the calculation of the shielding effectiveness (SE) of a large metallic enclosure with small openings is complicated. Therefore, many approximate and exact numerical methods have been introduced. Highly accurate analytical approximate methods have been only applied on simple geometries. A simple analytical method was introduced by Robinson et al. based on a transmission line model [1, 2]. In this method, a rectangular enclosure was modeled by a short-circuited rectangular waveguide while a coplanar strip transmission line represented the aperture. In [3], an accurate model to predict the shielding effectiveness of a rectangular enclosure with numerous small apertures was presented. An appropriate equivalent admittance for the perforated side was suggested amid the free space and the enclosure, utilizing the traditional waveguide circuit model where the enclosure was represented by a short-circuited rectangular waveguide. Park and Eom [4] studied the electromagnetic wave penetration into a rectangular cavity with multiple rectangular apertures. The Fourier transform and mode matching were used to obtain simultaneous equations for the modal coefficients. The simultaneous equations were solved to represent the cavity field in series forms, which were suitable for numerical computations.

In addition to approximate analytical techniques, a number of numerical methods, such as transmission line modeling method time Domain (TLM-TD) [5], the method of moments (MOM) and integral equations [6], finite element method (FEM) [7], and finite difference time domain (FDTD) technique [8–10] have been proposed for the solution of shielding problems. In most of the above

Received 27 July 2020, Accepted 26 October 2020, Scheduled 28 October 2020

* Corresponding author: Hassan A. Ragheb (assan.ragheb@bue.edu.eg).
The author is with the Department of Electrical Engineering, The British University in Egypt, El Sherouk City, Misr-Ismaillia Road, Egypt.

mentioned methods, the effect of the perforated wall thickness is ignored to simplify the calculation. However, wall thickness has a significant impact on the SE of the perforated enclosure.

There are analytical approaches such as [11] in which the closed form expressions are derived for predicting energy leakage through a reflector surface or [12] where the semi-analytical MoM technique is utilized for several parallel thick plates with apertures. Radiation from a dielectric-loaded multi-slotted cylinder with thickness illuminated by electric or magnetic line source is formulated by using radial mode matching technique [13, 14]. The radiated and guided fields are represented in terms of an infinite series of radial modes. By applying the appropriate boundary conditions, the coefficients of radiated and guided fields are obtained.

In this paper, we investigate the shielding effectiveness of an infinitely long cylindrical enclosure of any cross-section simulated by metallic strips coated with dielectric material. A line source is placed inside the simulated cylindrical surface which illuminates the N dielectric coated conducting strips. Exact solution based on full wave analysis is developed to obtain the scattered field outside the simulated cylindrical surface. Fields outside the cylindrical surface are represented in terms of infinite series of Mathieu functions [15]. Multiple interactions of electromagnetic waves among the dielectric coated conducting cylinders are considered [16, 17]. The shielding effectiveness is then calculated at a far point as the ratio between the far fields of a line source in the presence of the simulated surface and in the absence of the surface. Numerical examples for circular and rectangular cross-sectional surfaces are presented.

2. FORMULATION OF THE PROBLEM

Figure 1 shows the cross section of a line source of intensity I_o placed at (ρ_o, ϕ_o) with respect to the global coordinate system (x, y, z). Cross sections of N dielectric coated conducting strips, of infinite length with their axes parallel to the z-axis, are placed on a trajectory of an arbitrary cross-sectional cylindrical surface around the line source. The ith conducting strip has a width $2d_i$ and coated with a dielectric substance of permittivity ε_i. The dielectric coating forms an elliptical structure. The focal length of the outer surface of the ith strip dielectric coating is equal to the conducting strip width while its semi-major axis and semi-minor axis are respectively denoted by a_i and b_i. The center of the ith dielectric coated strip is located at (r_i, ψ_i) with respect to the global coordinate system. The ith coated strip is inclined by an angle β_i with respect to the x-axis. In addition to the global coordinate system, N coordinate systems are defined at the coated strip centers such that the cross-sectional plane of the ith strip lies in the x_i-y_i plane.

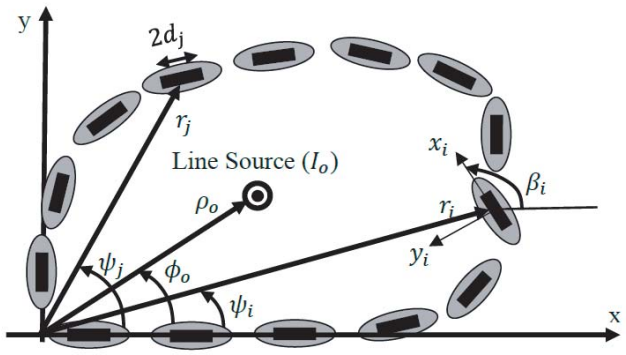

Figure 1. Geometry of the problem.

Consider a line source of intensity I_o placed at (ρ_0, ϕ_0) with respect to the global coordinates. The incident electric field by the line source is given by:

$$E_z^{inc} = \frac{\Omega}{4} H_0^{(1)} \left(k_0 \left| \rho - \rho_0 \right| \right) \tag{1}$$

where $\Omega = -\frac{k_0^2 I_o}{\omega\epsilon} = -k_o\eta_o I_o$. The z-polarized incident wave, with $e^{j\omega t}$ time dependence, is incident on the N dielectric coated strips. The z-component of the electric field due to the line source can be expanded in terms of Mathieu functions as:

$$E_z^{inc} = \Omega\left[\sum_{m=0}^{\infty}\frac{Se_m(h,\eta_0)}{N_m^{(e)}(h)}Se_m(h,\eta)\begin{cases} Je_m(h,\zeta_0)\,He_m^{(1)}(h,\zeta) & u>u_0 \\ Je_m(h,\zeta)\,He_m^{(1)}(h,\zeta_0) & u<u_0\end{cases}\right.$$
$$\left.+\frac{So_m(h,\eta_0)}{N_m^{(o)}(h)}So_n(h,\eta)\begin{cases} Jo_m(h,\zeta_0)\,Ho_m^{(1)}(h,\zeta) & u>u_0 \\ Jo_m(h,\zeta)\,Ho_m^{(1)}(h,\zeta_0) & u<u_0\end{cases}\right] \tag{2}$$

where,

$$\zeta_0 = \left[\frac{1}{2}\left(\frac{\rho_0^2}{d^2}+1\right)+\left(\frac{1}{4}\left(\frac{\rho_0^2}{d^2}+1\right)^2-\frac{x'^2_0}{d^2}\right)^{\frac{1}{2}}\right]^{\frac{1}{2}}, \quad \eta_0 = \frac{x'_0}{\zeta_0 d}, \quad x'_0 = \rho_0\cos\phi_0, \quad y'_0 = \rho_0\sin\phi_0 \tag{3}$$

$Je_n(h,\zeta)$ and $Jo_n(h,\zeta)$ are respectively the even and odd modified Mathieu functions of the first kind and order $n(He_n^{(1)}(h,\zeta) = Je_n(h,\zeta) + jNe_n(h,\zeta))$. Also, $Se_n(h,\eta)$ and $So_n(h,\eta)$ are respectively the even and odd angular Mathieu functions of order n. $N_n^{(e)}(h)$ and $N_n^{(o)}(h)$ are normalized functions. The Mathieu functions arguments are $h_i = k_o d_i$, $\zeta_i = \cosh u_i$ and $\eta_i = \cos v_i$, where u_i and v_i are elliptical cylindrical coordinates defined by:

$$x_i = d_i\cosh u_i\cos v_i, \quad y_i = d_i\cosh u_i\sin v_i \tag{4}$$

The line source electric field can also be expressed in terms of (ρ_i,ϕ_i) of the local coordinates of the ith dielectric coated conducting strip as:

$$E_{zi}^{inc} = \Omega\left[\sum_{m=0}^{\infty}\frac{Se_m(h,\eta_{0i})}{N_m^{(e)}(h)}Se_m(h,\eta_i)\begin{cases} Je_m(h,\zeta_{0i})\,He_m^{(1)}(h,\zeta_i) & u_i>u_{0i} \\ Je_m(h,\zeta_i)\,He_m^{(1)}(h,\zeta_{0i}) & u_i<u_{0i}\end{cases}\right.$$
$$\left.+\frac{So_m(h,\eta_{0i})}{N_m^{(o)}(h)}So_m(h,\eta_i)\begin{cases} Jo_m(h,\zeta_{0i})\,Ho_m^{(1)}(h,\zeta_i) & u_i>u_{0i} \\ Jo_m(h,\zeta_i)\,Ho_m^{(1)}(h,\zeta_{0i}) & u_i<u_{0i}\end{cases}\right] \tag{5}$$

where

$$\rho_i = \sqrt{\rho_0^2 + r_i^2 - 2\rho_0 r_i\cos(\phi_0-\psi_i)} \tag{6}$$
$$\phi_i = 90 + \psi_i - \beta_i - \alpha_i \tag{7}$$
$$\alpha_i = \cos^{-1}\left[\frac{\rho_i^2 + r_i^2 - \rho_0^2}{2\rho_i r_i}\right] \tag{8}$$
$$\zeta_{0i} = \left[\frac{1}{2}\left(\frac{\rho_i^2}{d^2}+1\right)+\left(\frac{1}{4}\left(\frac{\rho_i^2}{d^2}+1\right)^2-\frac{x'^2_i}{d^2}\right)^{1/2}\right]^{1/2} \tag{9}$$
$$\eta_{0i} = \frac{x'_i}{\zeta_{0i}d}, \quad x'_i = \rho_i\cos\phi_i, \quad y'_i = \rho_i\sin\phi_i \tag{10}$$

The scattered electric field from the ith coated strip can be expressed in terms of the local coordinates at the center of each coated strip. Region (I) lies inside the dielectric coating while region (II) lies outside the dielectric coating. The scattered field from the ith strip in region (I) is given by:

$$E_{z_i}^{(I)} = \Omega\sum_{n=0}^{\infty}A_n^{(i)}\left\{Je_n(H_i,\zeta_i) - \frac{Je_n(H_i,1)}{Ne_n^{(e)}(H_i,1)}Ne_n(H_i,\zeta_i)\right\}Se_n(H_i,\eta_i) \tag{11}$$

where $H_i = k_i d_i$ and $k_i = k_o\sqrt{\mu_{r_i}\varepsilon_{r_i}}$. $A_n^{(i)}$ are unknown coefficients to be calculated from the boundary conditions. The boundary condition of the vanishing tangential component of the electric field on the

conducting strip surface is satisfied in Eq. (11). The scattered field from the ith strip in region (II) is given by:

$$E_{z_i}^{(II)} = \Omega \sum_{n=0}^{\infty} B_n^{(i)} He_n^{(1)}(h_i\zeta_i) Se_n(h_i,\eta_i) \tag{12}$$

$B_n^{(i)}$ are unknown coefficients to be calculated from the boundary conditions of homogenous tangential components of electric and magnetic fields at the surface of the dielectric coatings, i.e.,

$$E_{z_i}^{inc} + \sum_{j=1}^{N} E_{z_j}^{(II)} = E_{z_i}^{(I)} \quad \text{on dielectric coating of } i\text{th element} \tag{13}$$

$$H_{z_i}^{inc} + \sum_{j=1}^{N} H_{z_j}^{(II)} = H_{z_i}^{(I)} \quad \text{on dielectric coating of } i\text{th element} \tag{14}$$

In order to apply the above boundary conditions, one has to transfer the electric and magnetic field expressions from one coordinate system to the other. This can be done using the addition theorem of the Mathieu functions, namely

$$\begin{aligned} He_m(a_q,\zeta_q)\, Se_m(a_q,\eta_q) \;=\; & \sum_{n=0}^{\infty} U_{n,m}(l,q)\, Je_n(a_l,\zeta_l)\, Se_n(a_l,\eta_l) \\ & + \sum_{n=1}^{\infty} E_{n,m}(l,q)\, Jo_n(a_l,\zeta_l)\, So_n(a_l,\eta_l) \end{aligned} \tag{15}$$

where

$$U_{n,m}(l,q) \;=\; \frac{\pi(j)^{n-m}}{N_n^{(e)}(a_l)} \sum_{i=0}^{\infty}\sum_{p=0}^{\infty} (j)^{-i-p}\, De_p^n(a_l)\, De_i^n(a_q)\, Be_{i,p} \tag{16}$$

$$E_{n,m}(l,q) \;=\; \frac{\pi(j)^{n-m-1}}{2N_n^{(o)}(a_l)} \sum_{i=0}^{\infty}\sum_{p=0}^{\infty} \epsilon_i\,(j)^{-i-p} Do_p^n(a_l)\, De_i^n(a_q)\, Be_{i,p} \tag{17}$$

And

$$Be_{i,p} \;=\; H_{p-i}^{(1)}(ks_{lq})\cos(p\psi_{lq} - i\psi_{ql}) + (-1)^i H_{p+i}^{(1)}(ks_{lq})\cos(p\psi_{lq} + i\psi_{ql}) \tag{18}$$

$$\psi_{ik} \;=\; \tan^{-1}\left[\frac{y_k - y_i}{x_k - x_i}\right] - \beta_i \tag{19}$$

$$S_{ik} \;=\; \sqrt{(x_i - x_k)^2 + (y_i - y_k)^2} \tag{20}$$

Employing Eq. (15) in Eq. (12)

$$\begin{aligned} E_{z_j}^{(II)} \;=\; & \Omega \sum_{n=0}^{\infty} B_n^{(j)} \left[\sum_{k=0}^{\infty} U_{k,n}(i,j)\, Je_k(h_i,\zeta_i)\, Se_k(h_i,\eta_i)\right. \\ & \left. + \sum_{k=1}^{\infty} E_{k,n}(i,j)\, Jo_k(h_i,\zeta_i)\, So_k(h_i,\eta_i)\right] \end{aligned} \tag{21}$$

Applying the boundary condition in Eq. (13) and multiplying both sides of the resulting equation by

$Se_m(H_i,\eta_i)$ then integrating over v_i from 0 to 2π, one obtains:

$$\begin{aligned}
&\sum_{n=0}^{\infty}\frac{Se_n\left(h_i,\eta_{0i}\right)}{N_n^{(e)}\left(h\right)}Je_n\left(h_i,\zeta_i\right)He_n^{(1)}\left(h_i,\zeta_{0i}\right)M_{n,m}\left(h_i,H_i\right)\\
&+\sum_{\substack{j=1\\ j\neq i}}^{N}\sum_{n=0}^{\infty}\sum_{k=0}^{\infty}B_n^{(j)}U_{k,n}\left(i,j\right)Je_k\left(h_i,\zeta_i\right)M_{k,m}\left(h_i,H_i\right)+\sum_{n=0}^{\infty}B_n^{(i)}He_n^{(1)}(h_i\zeta_i)M_{n,m}\left(h_i,H_i\right)\\
&=A_m^{(i)}\left\{Je_m\left(H_i,\zeta_i\right)-\frac{Je_m\left(H_i,1\right)}{Ne_m^{(e)}(H_i,1)}Ne_m\left(H_i,\zeta_i\right)\right\}N_m^{(e)}\left(H_i\right)
\end{aligned}\tag{22}$$

where

$$M_{n,m}\left(h_i,H_i\right)=\int_0^{2\pi}Se_n(h_i,\eta_i)Se_m\left(H_i,\eta_i\right)dv_i\tag{23}$$

The magnetic field component H_v can be obtained from:

$$H_v=\frac{-jk}{\omega\mu d\sqrt{\zeta^2-\eta^2}}\frac{\partial E_z}{\partial u}\tag{24}$$

Applying the boundary condition in Eq. (14), one obtains:

$$\begin{aligned}
&\frac{-jk_0}{\omega\mu d\sqrt{\zeta^2-\eta^2}}\left[\sum_{m=0}^{\infty}\frac{Se_m\left(h,\eta_{0i}\right)}{N_m^{(e)}\left(h\right)}Se_m\left(h,\eta_i\right)Je'_m\left(h,\zeta_i\right)He_m^{(1)}\left(h,\zeta_{0i}\right)\right.\\
&\left.+\frac{So_m\left(h,\eta_{0i}\right)}{N_m^{(o)}\left(h\right)}So_m\left(h,\eta_i\right)Jo'_m\left(h,\zeta_i\right)Ho_m^{(1)}\left(h,\zeta_{0i}\right)\right]\\
&+\frac{-jk_0}{\omega\mu d\sqrt{\zeta^2-\eta^2}}\sum_{\substack{j=1\\ j\neq i}}^{N}\sum_{n=0}^{\infty}\left[\sum_{k=0}^{\infty}B_n^{(j)}U_{k,n}\left(i,j\right)Je'_k\left(h_i,\zeta_i\right)Se_k\left(h_i,\eta_i\right)\right.\\
&\left.+\sum_{k=1}^{\infty}E_{k,n}\left(i,j\right)Jo'_k\left(h_i,\zeta_i\right)So_k\left(h_i,\eta_i\right)\right]\\
&+\frac{-jk_0}{\omega\mu d\sqrt{\zeta^2-\eta^2}}\sum_{n=0}^{\infty}B_n^{(i)}He_n^{(1)'}(h_i\zeta_i)Se_n\left(h_i,\eta_i\right)\\
&=\frac{-jk_i}{\omega\mu d\sqrt{\zeta^2-\eta^2}}\sum_{n=0}^{\infty}A_n^{(i)}\left\{Je'_n\left(H_i,\zeta_i\right)-\frac{Je_n\left(H_i,1\right)}{Ne_n^{(e)}(H_i,1)}Ne'_n\left(H_i,\zeta_i\right)\right\}Se_n\left(H_i,\eta_i\right)
\end{aligned}\tag{25}$$

where the prime indicates the derivative with respect to u.

Again, multiplying both sides of Equation (25) by $Se_m(H_i,\eta_i)$ and integrating over v_i from 0 to 2π, one obtains:

$$\begin{aligned}
&\sum_{n=0}^{\infty}\frac{Se_n\left(h,\eta_{0i}\right)}{N_n^{(e)}\left(h\right)}Je'_n\left(h,\zeta_i\right)He_n^{(1)}\left(h,\zeta_{0i}\right)M_{n,m}\left(h_i,H_i\right)\\
&+\sum_{\substack{j=1\\ j\neq i}}^{N}\sum_{n=0}^{\infty}\sum_{k=0}^{\infty}B_n^{(j)}U_{k,n}\left(i,j\right)Je'_k\left(h_i,\zeta_i\right)M_{k,m}\left(h_i,H_i\right)+\sum_{n=0}^{\infty}B_n^{(i)}He_n^{(1)'}\left(h_i,\zeta_i\right)M_{n,m}\left(h_i,H_i\right)\\
&=\sqrt{\varepsilon}_rA_m^{(i)}\left\{Je'_m\left(H_i,\zeta_i\right)-\frac{Je_m\left(H_i,1\right)}{Ne_m^{(e)}\left(H_i,1\right)}Ne'_m\left(H_i,\zeta_i\right)\right\}N_m^{(e)}\left(H_i\right)
\end{aligned}\tag{26}$$

From Eqs. (22) and (26), one can obtain

$$\begin{aligned}
&\sum_{n=0}^{\infty}\frac{Se_n\left(h_i,\eta_{0i}\right)}{N_n^{(e)}\left(h\right)}\left\{Je_n\left(h_i,\zeta_i\right)X'_m\left(H_i\right)-Je'_n\left(h,\zeta_i\right)X_m\left(H_i\right)\right\}He_n^{(1)}\left(h_i,\zeta_{0i}\right)M_{n,m}\left(h_i,H_i\right)\\
&=+\sum_{\substack{j=1\\ j\neq i}}^{N}\sum_{n=0}^{\infty}B_n^{(j)}\sum_{k=0}^{\infty}U_{k,n}\left(i,j\right)\left\{X_m\left(H_i\right)Je'_k\left(h_i,\zeta_i\right)-X'_m\left(H_i\right)Je_k\left(h_i,\zeta_i\right)\right\}M_{k,m}\left(h_i,H_i\right)\\
&+\sum_{n=0}^{\infty}B_n^{(i)}\Big\{X_m\left(H_i\right)He_n^{(1)'}\left(h_i,\zeta_i\right)-X'_m(H_i)He_n^{(1)}(h_i,\zeta_i)\Big\}M_{n,m}\left(h_i,H_i\right)
\end{aligned}\tag{27}$$

where

$$X_m\left(H_i\right)=\left\{Je_m\left(H_i,\zeta_i\right)-\frac{Je_m\left(H_i,1\right)}{Ne_m^{(e)}\left(H_i,1\right)}Ne_m\left(H_i,\zeta_i\right)\right\}N_m^{(e)}\left(H_i\right)\tag{28}$$

$$X'_m\left(H_i\right)=\sqrt{\varepsilon}_r\left\{Je'_m\left(H_i,\zeta_i\right)-\frac{Je_m\left(H_i,1\right)}{Ne_m^{(e)}\left(H_i,1\right)}Ne'_m\left(H_i,\zeta_i\right)\right\}N_m^{(e)}\left(H_i\right)\tag{29}$$

Equation (27) must be applied on all elements from $i=1$ to $i=N$, and it can then be written in a matrix form, i.e.,

$$\begin{bmatrix} C_{m,n}^{(11)} & C_{m,n}^{(12)} & . & . & C_{m,n}^{(1N)}\\ C_{m,n}^{(21)} & . & . & . & C_{m,n}^{(2N)}\\ . & . & . & . & .\\ . & . & . & . & .\\ C_{m,n}^{(N1)} & C_{m,n}^{(N2)} & . & . & C_{m,n}^{(NN)} \end{bmatrix}\begin{bmatrix} B_n^{(1)}\\ B_n^{(2)}\\ .\\ .\\ B_n^{(N)} \end{bmatrix}=\begin{bmatrix} Z_m^{(1)}\\ Z_m^{(2)}\\ .\\ .\\ Z_m^{(N)} \end{bmatrix}\tag{30}$$

where

$$\begin{aligned}
Z_m^i&=\sum_{n=0}^{\infty}\frac{Se_n\left(h_i,\eta_{0i}\right)}{N_n^{(e)}\left(h\right)}\left\{Je_n\left(h_i,\zeta_i\right)X'_m\left(H_i\right)\right.\\
&\left.-Je'_n\left(h,\zeta_i\right)X_m\left(H_i\right)\right\}He_n^{(1)}\left(h_i,\zeta_{0i}\right)M_{n,m}\left(h_i,H_i\right)
\end{aligned}\tag{31}$$

$$C_{m,n}^{ii}=\Big\{X_m\left(H_i\right)He_n^{(1)'}\left(h_i,\zeta_i\right)-X'_m(H_i)He_n^{(1)}(h_i,\zeta_i)\Big\}M_{n,m}\left(h_i,H_i\right)\tag{32}$$

$$C_{m,n}^{ij}=\sum_{k=0}^{\infty}U_{k,n}\left(i,j\right)\left\{X_m\left(H_i\right)Je'_k\left(h_i,\zeta_i\right)-X'_m\left(H_i\right)Je_k\left(h_i,\zeta_i\right)\right\}M_{k,m}\left(h_i,H_i\right),\quad j\neq i\tag{33}$$

Once the unknown coefficients are calculated, the scattered field may be obtained via the relation:

$$E_z^{(s)}=\Omega\sum_{j=1}^{N}\sum_{n=0}^{\infty}B_n^{(j)}He_n^{(1)}(h_j,\zeta_j)Se_n\left(h_j,\eta_j\right)\tag{34}$$

Employing the asymptotic equation of the Mathieu function for the far field, namely

$$He_n^{(1)}\left(h_j,\zeta_j\right)=\frac{1}{\sqrt{h\zeta_j}}e^{j\left(h_j\zeta_j-\left(\frac{2n+1}{4}\right)\pi\right)}\tag{35}$$

one obtains

$$E_z^{(s)}=\Omega\sum_{j=1}^{N}\sum_{n=0}^{\infty}B_n^{(j)}\frac{1}{\sqrt{h_j\zeta_j}}e^{j\left(h_j\zeta_j-\left(\frac{2n+1}{4}\right)\pi\right)}Se_n\left(h_j,\eta_j\right)\tag{36}$$

and for large $h_j\zeta_j$ it can be represented in terms of circular cylindrical coordinates ($h_j\zeta_j=k_0\rho_j$).

For far field $\rho_j = \rho - r_j\cos(\phi - \psi_j)$, thus

$$E_z^{(s)} = \Omega\frac{e^{jk_0\rho}}{\sqrt{k_0\rho}}e^{-j\frac{\pi}{4}}\sum_{j=1}^{N}e^{-jk_0r_j\cos(\phi-\psi_j)}\sum_{n=0}^{\infty}(-j)^n B_n^{(j)}Se_n\left(h_j,\cos\phi_j\right) \tag{37}$$

Also, the incident electric field can be calculated at a far point by employing the following asymptotic equation

$$H_m^{(1)}\left(k_o\rho\right) = \frac{1}{\sqrt{k_o\rho}}e^{j\left(k_o\rho-\left(\frac{(2m+1)}{4}\right)\pi\right)} \tag{38}$$

Employing Eq. (38) in Eq. (1), one obtains

$$E_z^{inc} = \frac{\Omega}{4}\frac{1}{\sqrt{k_0\left|\rho-\rho_0\right|}}e^{j(k_0|\rho-\rho_0|-(\frac{\pi}{4}))} \tag{39}$$

Since for the far field $\rho \gg \rho_0$, thus

$$E_z^{inc} = \frac{\Omega}{4}\frac{e^{jk_0\rho}}{\sqrt{k_0\rho}}e^{-j(k_0\rho_0\cos\phi_0+\frac{\pi}{4})} \tag{40}$$

Shielding effectiveness is defined as

$$\begin{aligned} S_E(\phi) = &= -20\log\left|\frac{E_z^{(s)}\left(far\ field\right)}{E_z^{inc}\left(far\ field\right)}\right| \\ &= -20\log\left|4e^{jk_0\rho_0\cos\phi_0}\sum_{j=1}^{N}e^{-jk_0r_j\cos(\phi-\psi_j)}\sum_{n=0}^{\infty}(-j)^n B_n^{(j)}Se_n\left(h_j,\cos\phi_j\right)\right| \end{aligned} \tag{41}$$

3. RESULTS AND DISCUSSION

A computer program developed to calculate the shielding effectiveness of a closed cylindrical surface is simulated by N dielectric coated conducting strips. To check the accuracy of our program, the special case of the radiated field versus frequency through a slotted circular cylinder with the electric line current at cylinder center is considered. Results of this special case have been published by Lee el al. [13]. The radius of the circular cylinder $b = 1\,\text{m}$ and the sectoral angle of the slot is 60°. The cylindrical surface is simulated by 20 conducting strips, and each has a width of 0.2 m. Fig. 2 illustrates the radiated electric field pattern based on our calculations which is compared with the published data in [13]. Excellent agreement between our work and the published work is found as can be seen from Fig. 2, which gives us confidence in our calculations.

The first case we present is for the calculation of the shielding effectiveness of a closed circular cross-sectional cylindrical surface of radius $1\lambda_0$ simulated by 20 dielectric coated conducting strips. The electric line source placed at different positions inside the cylinder is shown in Fig. 3. The geometrical parameters are $d = 0.1\lambda_0$, $a = 0.11\lambda_0$ and $\varepsilon_r = 2.3$. As one can see from Fig. 3, shielding effectiveness pattern will be more directive in the direction of larger off-center displacement of the electric line source from the cylindrical surface axis. Shielding effectiveness in this case has a maximum value of 3.6 dB and minimum value of 1.3 dB. An application of this example may be considered as a shielded room with sensitive equipment that should be shielded from any outside electromagnetic waves. The results shown in Figure 3 also show the sensitivity of the shielding effectiveness with respect to the position inside the shielded room.

The second example presented here is for a shielding effectiveness of square cross-sectional cylindrical surface, of side length $1.92\lambda_0$. The cylindrical surface in this case is simulated by 32 dielectric coated conducting strips. Shielding effectiveness pattern for this geometry is calculated for three different dielectric coating thicknesses. Fig. 4, illustrates the shielding effectiveness pattern around the shielding surface for $d = 0.1\lambda_0$ and $\varepsilon_r = 2.3$. As can be seen from Fig. 4, the shielding effectiveness is almost the same for different dielectric coating thicknesses except that at the square corners it increases with the thickness of the dielectric coating. The shielding effectiveness around this cylindrical surface varies

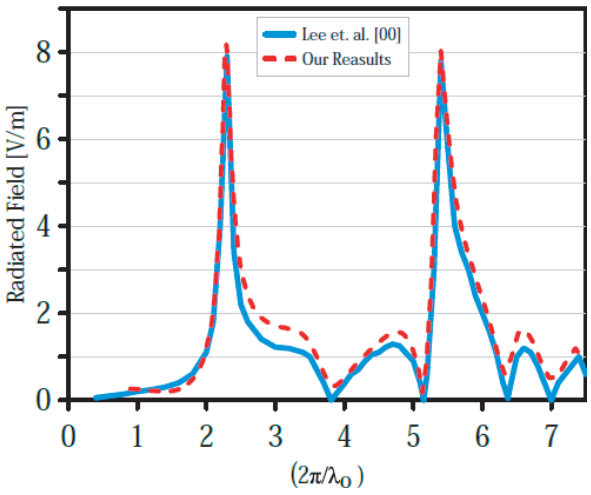

Figure 2. The radiated field versus frequency through slotted circular cylinder with electric line current at the center and slot angle 60°.

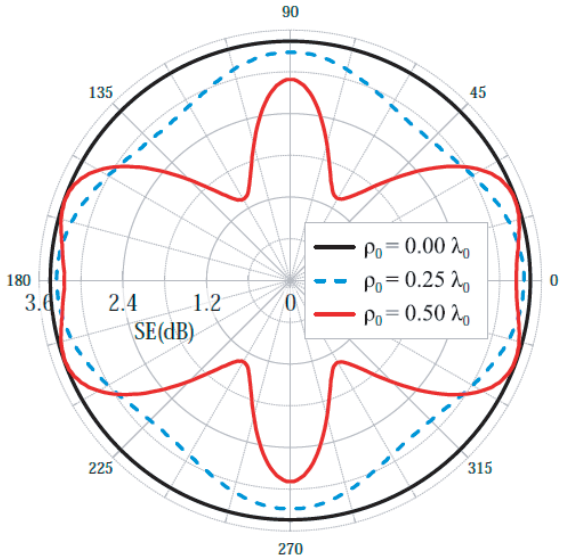

Figure 3. Shielding effectiveness of a circular cylindrical surface simulated by 20 dielectric coating conducting strips.

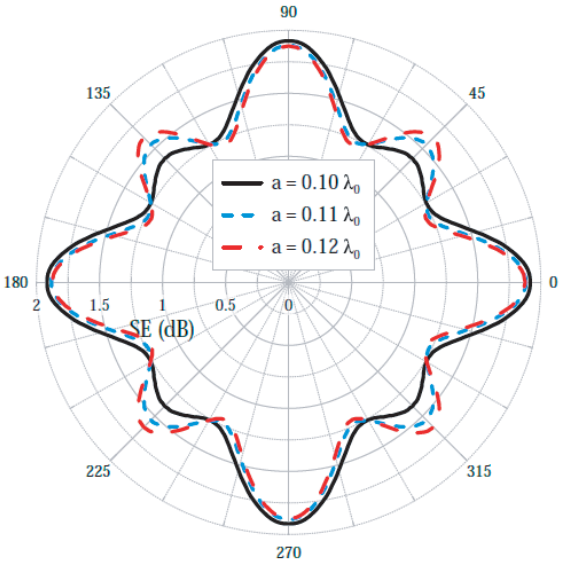

Figure 4. Shielding effectiveness of a cylindrical surface of square cross-section simulated by 32 dielectric coating conducting strips of different coating thickness.

between 2.4 dB and 4 dB. Accordingly, in designing a square shielding room one must choose reasonable dielectric thickness to increase the shielding effectiveness along the corner directions.

For the third example, we have considered the same geometrical parameters of the simulated square cross-sectional surface. However, shielding effectiveness was calculated for three different dielectric permittivities. Fig. 5 shows the shielding effectiveness pattern around the shielding surface for $d = 0.1\lambda_0$ and $a = 0.11$. As can be seen from Fig. 5, the shielding effectiveness is almost the same for different dielectric coating permittivities except that at the square corners it increases with the increase of the dielectric permittivity. The shielding effectiveness around this cylindrical surface varies between 2.5 dB and 3.8 dB. Shielding effectiveness pattern is rarely calculated in similar studies. The results presented so far have considered a single frequency, and in order to see the effect of the frequency on the shielding effectiveness the following example is considered.

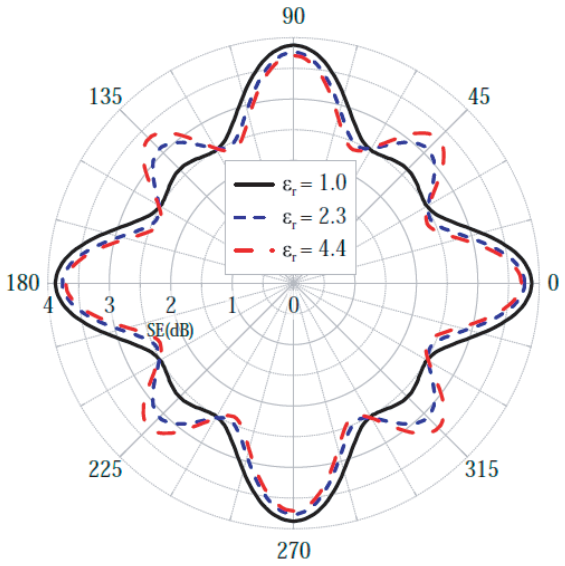

Figure 5. Shielding effectiveness of a cylindrical surface of square cross-section simulated by 32 dielectric coating conducting strips of different ε_r.

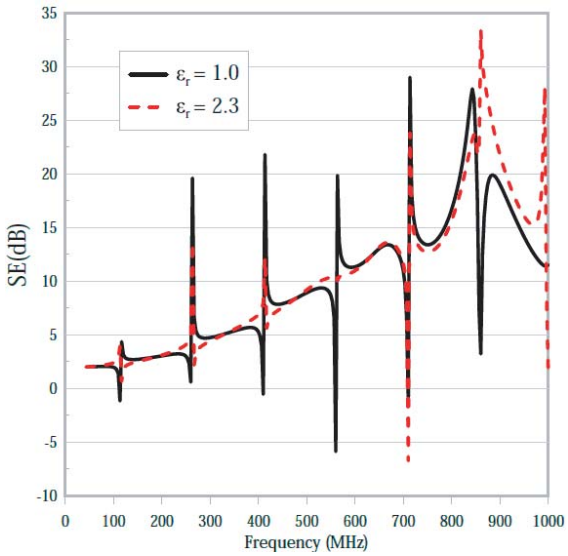

Figure 6. Shielding effectiveness of circular cylindrical surface versus frequency.

Finally, shielding effectiveness of a circular cylindrical surface of radius $1\lambda_0$ simulated by 20 dielectric coated conducting strips of $d = 0.1\lambda_0$ and $a = 0.11\lambda_0$ is calculated at different frequencies as shown in Fig. 6. Two cases are presented in Fig. 6. The first is for $\varepsilon_r = 1$ while the second is for $\varepsilon_r = 2.3$. As can be noticed from Fig. 6, the shielding effectiveness is increased as the frequency increases. In addition, in both cases there are many frequencies at which resonance occurs corresponding to different modes inside the circular waveguide. For the case of simulation with conducting strips ($\varepsilon_r = 1$), resonance frequencies occur at 114.82 MHz, 263.56 MHz, 413.18 MHz, 563 MHz, 712.9 MHz, 862.82 MHz, corresponding to TM_{01}, TM_{02}, TM_{03}, TM_{04}, TM_{05}, and TM_{06}, respectively. The importance of this result lies in predicting resonance frequencies in order to avoid them when this shielding is used.

4. CONCLUSION

Studying the shielding effectiveness of a cylindrical surface by N dielectric coated conducing strips is achieved. Shielding a room can be done by placing conducting strips in the trajectory to cylindrical cross section. Two major examples are presented here. The first is for a circular cylindrical surface while the second is for a square cross-sectional cylindrical surface. In both cases, shielding effectiveness pattern outside the shielding surface can be calculated and optimized to any desired value. In addition, this study shows that shielding effectiveness swings from very low value to very high value at TM_{0n} cutoff frequencies of circular cross-sectional cylindrical surface. Therefore, for room shielding resonance frequencies must be avoided.

ACKNOWLEDGMENT

The author wishes to acknowledge ***the British University in Egypt*** for providing all the facilities and the financial assistance required to perform this research.

REFERENCES

1. Robinson, M. P., J. D. Turner, D. W. P. Thomas, J. F. Dawson, M. D. Ganley, A. C. Marvin, S. J. Porter, T. M. Benson, and C. Christopoulos, "Shielding effectiveness of a rectangular enclosure with a rectangular aperture," *Electronics Letters*, Vol. 32, No. 17, 1559–1560, Aug. 1996.

2. Robinson, M. P., T. M. Benson, C. Christopoulos, J. F. Dawson, M. D. Ganley, A. C. Marvin, S. J. Porter, and D. W. P. Thomas, "Analytical formulation for the shielding effectiveness of enclosures with apertures," *IEEE Trans. Electromagn. Compat.*, Vol. 40, No. 3, 240–248, Aug. 1998.
3. Dehkhoda, P., A. Tavakoli, and R. Moini, "An efficient and reliable shielding effectiveness evaluation of a rectangular enclosure with numerous apertures," *IEEE Trans. Electromag. Compat.*, Vol. 50, No. 1, 208–212, Feb. 2008.
4. Park, H. H. and H. J. Eom, "Electromagnetic penetration into a rectangular cavity with multiple rectangular apertures in a conducting plane," *IEEE Trans. Electromag. Compat.*, Vol. 42, No. 3, 303–307, Aug. 2000.
5. Bahadorzadeh Ghandehari, M., M. Naser-Moghaddasi, and A. R. Attari, "Improving of shielding effectiveness of a rectangular metallic enclosure with aperture by using extra wall," *Progress In Electromagnetics Research Letters*, Vol. 1, 45–50, 2008.
6. Wallyn, W., D. De Zutter, and H. Rogier, "Prediction of the shielding and resonant behavior of multisection enclosures based on magnetic current modeling," *IEEE Trans. Electromag. Compat.*, Vol. 44, No. 1, 130–138, Feb. 2002.
7. Edrisi, M. and A. Khodabakhshian, "Simple methodology for electric and magnetic shielding effectiveness computation of enclosures for electromagnetic compatibility use," *Journal of Electromagnetic Waves and Applications*, Vol. 20, No. 8, 1051–1060, 2006.
8. Jiao, C., X. Cui, L. Li, and H. Li, "Subcell FDTD analysis of shielding effectiveness of a thin-walled enclosure with an aperture," *IEEE Trans. Magnetics*, Vol. 42, No. 4, 1075–1078, Apr. 2006.
9. Li, M., K. P. Ma, D. M. Hockanso, J. L. Drewniak, T. H. Hubing, and T. P. Van Doren, "Numerical and experimental corroboration of an FDTD thin-slot model for slots near corners of shielding enclosures," *IEEE Trans. Electromag. Compat.*, Vol. 39, No. 3, 225–232, 1997.
10. Edelvik, F. and T. Weiland, "Stable modeling of arbitrarily oriented thin slots in the FDTD method," *IEEE Trans. Electromag. Compat.*, Vol. 47, No. 3, 440–446, Aug. 2005.
11. Chen, C. C., "Transmission of microwave through perforated flat plates of finite thickness," *IEEE Trans. Microwave. Theory Tech.*, Vol. 21, No. 1, 1–6, Jan. 1973.
12. Wallyn, W., D. De Zutter, and E. Laermans, "Fast effectiveness prediction for realistic rectangular enclosure," *IEEE Trans. Electromag. Compat.*, Vol. 45, No. 4, 639–643, Nov. 2003.
13. Lee, W.-S., H.-L. Lee, H.-S. Jang, H.-S. Tae, and J.-W. Yu, "Analysis of scattering with multi-slotted cylinder with thickness: TM case," *Progress In Electromagnetics Research*, Vol. 128, 105–120, 2012.
14. Jang, H.-S., W.-S. Lee, H.-S. Tae, H.-L. Lee, and J.-W. Yu, "Transmission and shielding from a magnetic line current placed inside or outside of the multi-slotted circular cylinder," *Journal of Electromagnetic Waves and Applications*, Vol. 26, Nos. 11–12, 1507–1520, Aug. 2012.
15. Holland, R. and V. Cable, "Mathieu function and their applications to scattering by a coated strip," *IEEE Trans. Electromag. Compat.*, Vol. 34, 9–16, Feb. 1992.
16. Sebak, A., "Electromagnetic scattering by two elliptic cylinders," *IEEE Antennas and Propag.*, Vol. 42., No. 11, 1521–1527, 1994.
17. Ragheb, H. and E. Hassan, "Plane wave scattered by N dielectric coated conducting strips," *IET Microwave, Antennas and Propagation*, Vol. 6, No. 8, 938–944, 2012.